

University of Groningen

## Regional diversity in oligodendrocyte progenitor cells

Lentferink, Dennis Hendrikus

DOI:  
[10.33612/diss.165785295](https://doi.org/10.33612/diss.165785295)

**IMPORTANT NOTE: You are advised to consult the publisher's version (publisher's PDF) if you wish to cite from it. Please check the document version below.**

*Document Version*  
Publisher's PDF, also known as Version of record

*Publication date:*  
2021

[Link to publication in University of Groningen/UMCG research database](#)

*Citation for published version (APA):*

Lentferink, D. H. (2021). *Regional diversity in oligodendrocyte progenitor cells: implications for remyelination in grey and white matter*. [Thesis fully internal (DIV), University of Groningen]. University of Groningen. <https://doi.org/10.33612/diss.165785295>

### Copyright

Other than for strictly personal use, it is not permitted to download or to forward/distribute the text or part of it without the consent of the author(s) and/or copyright holder(s), unless the work is under an open content license (like Creative Commons).

The publication may also be distributed here under the terms of Article 25fa of the Dutch Copyright Act, indicated by the "Taverne" license. More information can be found on the University of Groningen website: <https://www.rug.nl/library/open-access/self-archiving-pure/taverne-amendment>.

### Take-down policy

If you believe that this document breaches copyright please contact us providing details, and we will remove access to the work immediately and investigate your claim.

*Downloaded from the University of Groningen/UMCG research database (Pure): <http://www.rug.nl/research/portal>. For technical reasons the number of authors shown on this cover page is limited to 10 maximum.*

# Chapter 5

**Comparative transcriptomic profiling of *ex-vivo* isolated A2B5-positive cells reveals age-specific regional heterogeneity and diversity in cellular composition**



Dennis H. Lentferink, Astrid M. Alsema, Inge L. Werkman, Marissa L. Dubbelaar, Nieske Brouwer, Bart J. L. Eggen, and Wia Baron

Department of Biomedical Sciences of Cells & Systems, Section Molecular Neurobiology, University of Groningen, University Medical Center Groningen, Groningen, the Netherlands.

*(manuscript in preparation)*

**Abstract**

Remyelination, the endogenous repair process initiated upon demyelination, is more efficient in the grey matter than in the white matter and its overall efficiency is decreased upon aging. *Ex vivo* isolated cells using antibody A2B5 are able to remyelinate axons in experimental models when transplanted into a de- or dysmyelinated environment. Cell surface binding of antibody A2B5 is used to characterize *in vitro*, and positively select *ex vivo*, multiple cell types of the central nervous system (CNS), including oligodendrocyte progenitor cells, restricted glia progenitor cells, multipotential neural progenitor cells, astrocytes and neurons. Given the relevance of A2B5-positive cells for demyelinating diseases, here we set out to characterize the transcriptome of *ex vivo* isolated A2B5-positive cells from cortex and corpus callosum in the developing and adult rat CNS at postnatal day 7 (P7) and P250 respectively. At P7, the transcriptome of A2B5-positive cells substantially differed between cortex and corpus callosum, but much less so at P250. Gene ontology analysis of differentially expressed genes revealed that A2B5-positive cells from different regions may be involved in distinct cell processes. CNS cell type-specific marker expression and deconvolution revealed that the identity of A2B5-positive cells at the gene expression level was not confined to oligodendrocyte progenitor cells and glia restricted progenitors but also other CNS cell types, including endothelial cells at P7 and microglia at P250. Altogether our comparative transcriptional profiling indicate an age-specific regional heterogeneity as well as an age-specific diversity in cellular composition in *ex vivo* isolated A2B5-positive cells. Hence, regional heterogeneity and cellular diversity with age should be taken into account when investigating the role of A2B5-positive cells in remyelination.

**Introduction**

A growing number of studies indicate regional and functional heterogeneity in glial cells of the grey matter (GM) and white matter (WM). While oligodendrocytes<sup>28,34</sup> (OLGs), astrocytes<sup>29,176,219,329</sup> (reviewed in <sup>436</sup>) and microglia<sup>478,486</sup> display transcriptional regional heterogeneity, oligodendrocyte progenitor cells (OPCs) are transcriptionally similar in the resting brain and their diversity is limited to function<sup>44,144</sup>. Regional heterogeneity may have consequences for central nervous system (CNS) injury and repair<sup>20,29,37,144</sup> (reviewed in <sup>436</sup>) that is particularly reflected in remyelination, which is more efficient in GM than WM after cuprizone-induced demyelination<sup>24,25</sup> and in multiple sclerosis (MS) lesions<sup>26,27</sup>. Another factor that contributes to remyelination efficiency is age. While robust in young adult rodents, remyelination in WM becomes impaired with increasing age<sup>14,45,46</sup>. This has been attributed to decreased myelin debris clearance by microglia, impaired OPC recruitment and differentiation, the prolonged presence of pro-inflammatory cytokines, decreased metabolic function, and increased DNA damage<sup>14,47,487-490</sup>. Furthermore, adult OPCs are more resembling to mature OLGs than to neonatal OPCs, and have to revert to a more immature stage upon demyelination<sup>57</sup>. Whether these observations are also valid in GM lesions is currently not known. Given the long residency in their respective environment and their limited migratory capacity in the healthy brain, cells in the GM and WM may differentially age and accordingly be differently equipped to respond to demyelination and/or in their ability to remyelinate axons. However, a detailed comparison of adult OPCs in the GM and WM is still lacking.

Cells isolated from human and rat brain tissue based on A2B5 immunoreactivity at the cell surface (referred to as A2B5 or A2B5-positive cells) have remyelinating capacities when transplanted into the dysmyelinated and demyelinated rodent CNS<sup>47,64,491-494</sup>. The monoclonal antibody A2B5 was produced by immunization with chicken embryonic retinal cells<sup>63</sup> and, although produced to recognize neurons, antibody A2B5 was initially primarily used for the detection of OPCs and to discern type 1 from type 2 astrocytes *in vitro*<sup>66,67</sup>. Antibody A2B5 binds to complex c-series gangliosides, including GT<sub>3</sub>, GT<sub>1c</sub> and GQ<sub>1c</sub><sup>387</sup>, and recognizes the structure Neu<sub>5</sub>A- $\alpha$ 2 $\rightarrow$ 8Neu<sub>5</sub>A- $\alpha$ 2 $\rightarrow$ 8Neu<sub>5</sub>A- $\alpha$ . This structure is not only present on gangliosides, but also on glycoproteins that are transiently present during mouse

CNS development under expression of the enzyme ST8Sia III<sup>495,496</sup>. Although the A2B5 epitope is present inside various cells of the CNS, it is specifically enriched on the cell surface of progenitor cells prompting antibody A2B5 to be a progenitor cell marker *in vitro*. Because of cell permeabilization, and thus exposure of intracellular A2B5 epitopes, immunostaining of rat CNS tissue with A2B5 results in staining of a variety of cells<sup>126</sup>. To date, antibody A2B5 has been used to isolate and characterize CNS cells from fetal and adult human and rodent brain tissue, *in vitro* and *in vivo*, including rat and human OPCs<sup>47,64,493,497,498</sup>, rat and human glia progenitor cells<sup>499–501</sup>, human multipotential neural progenitor cells<sup>492</sup>, murine neurons in early development<sup>65</sup>, human and rat astrocytes<sup>67,499,502</sup> and human glioblastoma cells<sup>503,504</sup>.

Given their remyelinating potential, A2B5-positive cells are of relevance for demyelinating diseases, including MS. Whether A2B5-positive cells are regionally different, whether this is affected by aging, and how this may relate to regional differences in remyelination efficiency remains to be determined. Here we set out to transcriptionally characterize and compare *ex vivo* isolated A2B5-positive cells from the cortex (cx, GM) and corpus callosum (cc, WM) of neonatal and middle-aged rat brain. Our findings revealed that at the transcriptional level A2B5-positive cells are a mixed population of CNS cell types of which the relative proportions considerably differ between neonatal and middle-aged rats. At the same age, relative cell type proportions of A2B5-positive cells only showed minor differences between cx and cc. Here, an age-specific transcriptomic heterogeneity was observed between A2B5-positive cells of the cx and cc. Hence, diversity in cell type proportions at different ages and transcriptomic heterogeneity between region at the same age, may underlie the functional differences in their contribution to remyelination.

## Results

### Regional transcriptomic variation in A2B5-positive cells diminishes with age

Regeneration of myelin is more efficient in demyelinated lesions of the GM than in lesions of the WM, both in MS<sup>26,27</sup> and in an experimental rodent model for de- and remyelination<sup>24,25</sup>. Cells identified by the binding of A2B5 can remyelinate the de- and dysmyelinated rodent CNS<sup>64,491–494</sup>. To investigate putative differences between A2B5-positive cells from GM and WM and the role of aging in different brain regions,

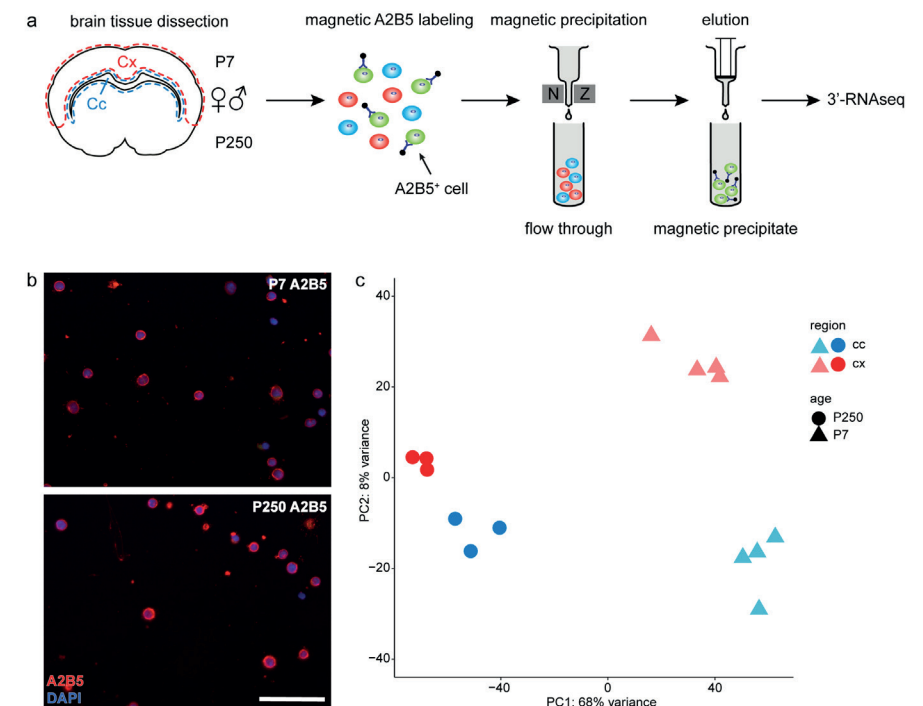


**Figure 1.** Regional transcriptomic variation in A2B5-positive cells diminishes with age. A2B5-positive cells (A2B5) were freshly isolated from the cortex (cxA2B5) and corpus callosum (ccA2B5) from postnatal days 7 (P7) and 250 (P250) rats using magnetic beads coupled to antibody A2B5. Antibody A2B5 binds c-series gangliosides and glycoproteins expressing the structure Neu5Acalpha2-->8Neu5Acalpha2-->8Neu5Acalpha-->. Four (P7) and three (P250) biological replicates of either region were subjected to bulk 3'-RNA sequencing. (a) Schematic representation of dissected areas and experimental set up to obtain *ex vivo* isolated cxA2B5 and ccA2B5. (b) Representative images of cells from the P7 and P250 brain stained with A2B5 (red) 1 hour after plating on poly-L-lysine coated coverslips. Nuclei are stained with DAPI (blue). (c) Principal component analysis (PCA) reveals that most variation in gene expression (68%; PC1, x-axis) exists between samples from the P7 and P250 group, while 8% (PC2, y-axis) seems associated with the regional origin. Scale bar is 50  $\mu$ m.

we performed bulk 3'-end RNA sequencing (3'-RNAseq) on the RNA of cells directly isolated from cortex (cxA2B5) and corpus callosum (ccA2B5) of neonatal (P7) and middle-aged (P250) rats using A2B5-coupled magnetic beads (Fig. 1a). At P7, i.e., just before the onset of myelination, postnatal OPC distribution from different oligodendrogenesis waves approach a steady state<sup>60</sup> and start to diverge, while still present at relatively high numbers. P250 in rat resembles a human age of approx. 25 years when myelination is complete and demyelinating diseases may manifest<sup>61,62</sup>. In addition, at P250 (re)myelination efficiency in WM is declined<sup>14,46</sup>. The obtained cell populations of either region and age contained approx. 94-97% A2B5-positive cells as quantified by A2B5 immunostaining 1 hour after plating on poly-L-lysine-coated glass coverslips (Fig. 1b). Principal component analysis (PCA) revealed that biological replicates segregated in relation to age and region, and that the majority of variation in gene expression (68%) between samples was associated with age, while 8% of variation was related to their region of origin (Fig. 1c). Furthermore, more variation was observed between the P7 cxA2B5 and ccA2B5 groups than between the P250 cxA2B5 and ccA2B5 samples (Fig. 1c). Hence, the transcriptomic profile of A2B5-positive cells is drastically changed with age, while the variation between region is only substantial at P7.

### A2B5-positive cells express a variety of CNS cell type-specific genetic markers which differ between region and age

Although mainly used as a marker for OPCs, antibody A2B5 has been used to identify and characterize multiple cell types. Therefore, we first compared the transcriptional levels of CNS cell type-specific marker genes in the different A2B5 samples. Transcripts of OLG lineage cell (OLC) markers *Olig1*, *Olig2* and *Sox10* were present in A2B5-positive cells. *Olig1* transcripts were more abundant in P7 A2B5 samples, both in cx and cc, while *Olig2* transcripts were more abundant in P7 cxA2B5, but not ccA2B5 (Fig. 2a). The abundance of transcripts for *Sox10* was similar in P7 and P250 A2B5 of both cx and cc (Fig. 2a). This indicates that the gene expression of OLG lineage markers was comparable between cx and cc of the same age, while being less abundant in P250 compared to P7 A2B5. The immature astrocyte (imASTR) marker *Fabp7* and the mature astrocyte (ASTR) markers *Aqp4* and *Gfap* were more abundantly expressed in P7 than in P250 cx samples (Fig. 2a). Transcripts of *Fabp7*

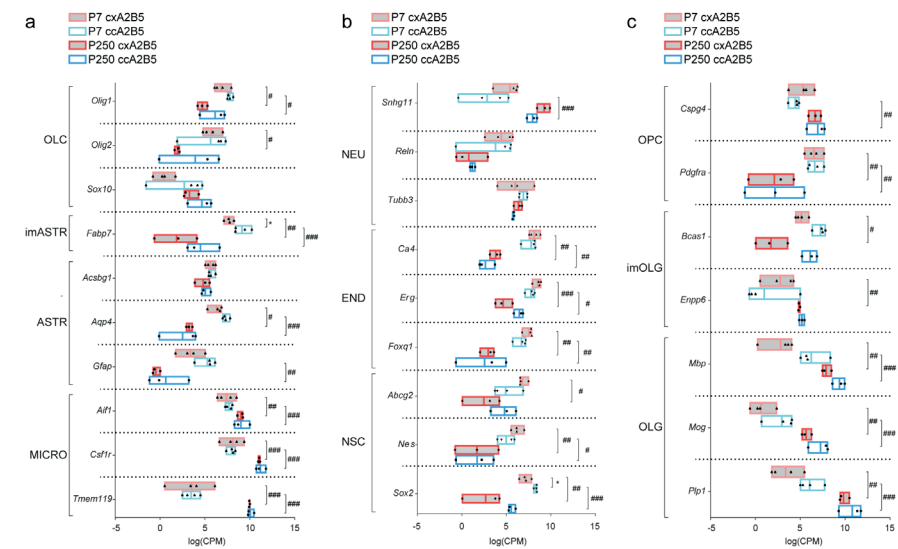


**Figure 2.** A2B5-positive cells express a variety of CNS cell type markers which differs with age. A2B5-positive cells (A2B5) were freshly isolated from the cortex (cxA2B5) and corpus callosum (ccA2B5) from postnatal days 7 (P7) and 250 (P250) rats using magnetic beads coupled to antibody A2B5. Antibody A2B5 binds c-series gangliosides and glycoproteins expressing the structure Neu5Acalpha2-->8Neu5Acalpha2-->8Neu5Acalpha-->. Four (P7) and three (P250) biological replicates were subjected to bulk 3'-RNA sequencing. Abundance of various central nervous system-resident cell type specific genes is compared between region at the same age and between age at the same regions. Dots indicate individual data points (a-c). (a) Abundance of gene transcripts as the log value of the counts per million (log(CPM)) specific for oligodendrocyte lineage cells (OLC), immature astrocytes (imASTR), astrocytes (ASTR), and microglia (MICRO). Note that the microglia marker gene transcript abundance is increased in P250 A2B5 compared to P7 A2B5. (b) Abundance of gene transcripts specific for neurons (NEU), endothelial cells (END) and neural stem cells (NSC). Note that endothelial marker gene transcript abundance is decreased in P250 A2B5 compared to P7 A2B5. (c) Abundance of gene transcripts specific for OPCs, immature oligodendrocytes (imOLG) and mature oligodendrocytes (OLG). Note that the abundance of OLG-specific gene transcripts is increased in P250 A2B5.

and *Aqp4* were also more abundant in P7 compared to P250 cc samples. In addition, *Fabp7* was more abundantly expressed in P7 cc than P7 cx. The abundance of transcripts of astrocyte marker *Acsbg1* did not differ between groups (Fig. 2a). Notably, the astrocyte marker genes were as abundantly expressed as the OLG lineage marker genes. Rather unexpectedly, transcripts of microglia (MICRO) markers *Aifi*, *Csf1r* and *Tmem110* were also highly abundant in *ex vivo* isolated A2B5-positive cells. More specifically, all three microglia markers were more abundantly expressed in P250 than in P7 of both cx and cc, while no significant differences were found between cxA2B5 and ccA2B5 of the same age (Fig. 2a). Immunocytochemical analysis

on adherent P250 A2B5-positive cells 1 hour after *ex vivo* isolation, demonstrated that 87% of the A2B5-positive cells co-labeled with the microglia-specific marker *Iba1* (*Aifi*), indicating that antibody A2B5 bound to microglia at P250 (Fig. S1). In addition to OLG lineage, astrocyte and microglia marker genes, neuronal (NEU), endothelial cells (END) and neural stem cell (NSC) markers were abundantly expressed in A2B5-positive cells (Fig. 2b). While transcripts for neuronal marker *Snhg11* were more abundant in P250 ccA2B5 than in P7 ccA2B5, transcripts of other neuronal markers *Reln* and *Tubb3* were comparable between region and age (Fig. 2b). Endothelial cell markers *Ca4*, *Erg* and *Foxq1* were all more abundantly expressed in P7 A2B5 compared to P250 A2B5, while no significant difference between cxA2B5 and ccA2B5 at the same age was identified (Fig. 2b). Transcripts of neural stem cell markers *Abcg2*, *Nes* and *Sox2* were more abundant in P7 than P250 cx, while *Nes* and *Sox2* were also more abundantly expressed in P7 than in P250 cc (Fig. 2b). In addition, *Sox2* transcripts were more abundant in P7 cc than in cx (Fig. 2b). Hence, both endothelial and neural stem cells markers were more abundant in P7 than in P250 A2B5. Previous *in vitro* and *in vivo* findings revealed that OPCs in WM may be more mature than OPC in GM<sup>44,144</sup>. Therefore, we next assessed the abundance of markers that are specific to the three OPC differentiation states, OPCs, immature OLGs (imOLG) and mature OLGs (OLG). OPC marker *Cspg4* is more abundant in ccA2B5, but not cxA2B5, at P250 compared to P7 (Fig. 2c). In contrast, OPC marker *Pdgfra* was more abundantly expressed in A2B5-positive cells at P7 compared to P250 (Fig. 2c). While transcripts of the immature OLG (imOLG) marker *Bcas1* were more abundant in P7 cxA2B5 than in P250 cxA2B5, another imOLG marker, *Enpp6*, was more abundantly expressed in P7 ccA2B5 compared to P250 ccA2B5 (Fig. 2c). Transcripts of the mature OLG markers *Mbp*, *Mog* and *Plp1* were more abundant in P250 than in P7 at both regions with a trend of a higher abundance in cc compared to cx (Fig. 2c). Hence, alterations in the abundance of OPC differentiation marker genes in A2B5-positive cells were mainly observed with age rather than between regions, with OPC marker gene *Pdgfra* being more abundantly expressed in P7 A2B5, and mature OLG marker genes in P250 A2B5. The relatively high abundance of transcripts for other CNS-type specific genes in addition to OLG lineage genes indicates that *ex vivo* isolated A2B5-positive cells may be a heterogeneous group of cells. Therefore, we next aimed to characterize relative cell type composition of the A2B5-positive cells using deconvolution.

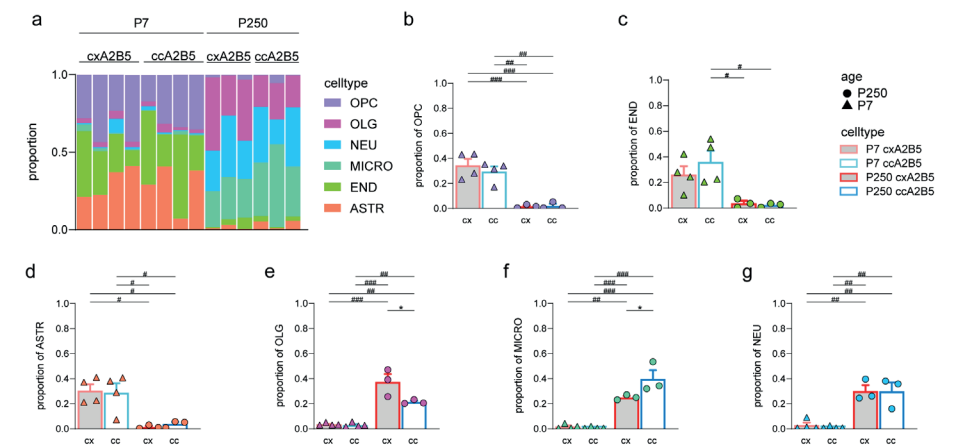


**Figure 3.** Deconvolution by BRETIGEA suggests that different CNS cell types are bound by antibody A2B5 at P7 and P250. A2B5-positives of cells (A2B5) were freshly isolated from the cortex (cxA2B5) and corpus callosum (ccA2B5) from postnatal days 7 (P7) and 250 (P250) rats using magnetic beads coupled to antibody A2B5. Antibody A2B5 binds c-series gangliosides and glycoproteins expressing the structure Neu5Acalpha2-->8Neu5Acalpha2-->8Neu5Acalpha-->. Four (P7) or three (P250) biological replicates were subjected to bulk 3'-RNA sequencing. Obtained data were deconvoluted using the R package BRETIGEA<sup>505</sup>. (a-g) Deconvolution of transcriptomic data using BRETIGEA to estimate the proportions of CNS cell types in bulk RNAseq samples, shown are the relative proportions per group (a). The average relative proportions of each cell type in the biological replicates are shown in b-g. Bars represent average relative proportion per group. Error bars indicate standard error of the mean (SEM). Dots represent individual data points. Statistical analysis was performed using a one-way ANOVA with a Tukey post-test to compare the relative cell proportion between all groups. P-values of <0.05, <0.01, and <0.001 were considered significant and indicated with \*, \*\* or \*\*\* respectively. Note that BRETIGEA reveals that irrespective of region P7 A2B5 consist of mostly oligodendrocyte progenitor cells (OPCs, a,b), endothelial cells (END, a,c) and astrocytes (ASTR, a,d), while P250 A2B5 consist mostly of oligodendrocytes (OLGs, a,e), microglia (MICRO, a,f), and neurons (NEU, a,g).

### A2B5-positive cells are a mixed population of cell types which differs with age

Deconvolution is a method that makes use of a panel of cell type-specific marker genes generated from single cell or single nucleus RNAseq studies to estimate the proportion of specific cell types in bulk RNAseq samples. To estimate the proportion of cell types in A2B5-bound samples, we first used BRETIGEA<sup>505</sup>, which calculates relative cell type proportions using a marker panel formed by multiple human and murine single-cell RNAseq datasets. Deconvolution by BRETIGEA indicated that P7 A2B5 were composed of approx. similar proportions of OPCs, endothelial cells and astrocytes both in cx and cc (Fig. 3a). The relative proportion of OLGs, microglia

and neurons in P7 A2B5 was minimal both in cx and cc (Fig. 3a). In contrast, both P250 cxA2B5 and P250 ccA2B5 contained approximately similar relative proportions of OLGs, microglia, and neurons (Fig. 3a), while OPCs, endothelial cells and astrocytes only had a minor contribution (Fig. 3a). Comparative analysis between regions revealed that the cellular proportions were similar between P7 cxA2B5 and P7 ccA2B5 (Fig. 3b-g). On the other hand, P250 ccA2B5 had a higher relative proportion of OLGs (Fig. 3e,  $p=0.013$ ) and lower relative proportions of microglia (Fig. 3f,  $p=0.032$ ) compared to P250 cxA2B5. As antibody A2B5 is known as a progenitor marker<sup>65,492,497,499</sup>, we also performed deconvolution by SCDC<sup>506</sup> using a murine single-cell dataset of Ximerakis and co-workers<sup>507</sup> that distinguishes 25 CNS cell types, including different types of progenitor cells (Fig. 4a). Using this dataset, 13 different cell types were identified in P7 A2B5, and only 6 distinct cell types in P250 A2B5. It was estimated that P7 A2B5 consisted mainly of endothelial cells (END) and neuronal restricted progenitors (NRP), with microglia contributing approximately 10% of cells and OPCs about 5% of cells (Fig. 4a-e). P250 A2B5 consisted of approx. 50% microglia (MICRO), 15% mature neurons (mNEUR), 15% neuroendocrine cells (NendC), and a marginal relative proportion of OLGs (0.8% cxA2B5, 6.4% ccA2B5) and astrocyte restricted progenitors (ARP) (0.4% cxA2B5, 1.6% ccA2B5) (Fig. 4a,d, f-i). Comparative analysis between regions at the same age revealed that the relative proportion of NRPs (Fig. 4c,  $p=0.002$ ), OPCs (Fig. 4e,  $p=0.021$ ) and ARPs (Fig. 4f,  $p=0.007$ ) was higher in P7 ccA2B5 compared to P7 cxA2B5, while in P250 ccA2B5 a lower proportion of NendC was observed compared to P250 cxA2B5 (Fig. 4h,  $p=0.027$ ). Hence, antibody A2B5-binding seems not to be restricted to OPCs, and the progenitor-like nature of A2B5-positive cells at P7 appeared to be lost at P250. To exclude that our findings depended on the isolation technique and the source of antibody A2B5, we next performed deconvolution on a publicly available bulk RNAseq dataset of *ex vivo* isolated A2B5-bound cells of young (P60-90) and aged (P600-730) whole adult rat brains<sup>47</sup>. Both deconvolution by BRETIGA and SCDC revealed that also in this data set in the adult brain microglia constituted a major cell proportion of A2B5-positive cells (Fig. S2). Hence, deconvolution suggests that surface A2B5-immunogenicity in the brain was not restricted to OPCs but rather to several cell types. At P7 this includes mainly progenitor cells, including OPCs, and endothelial cells, while at P250 this is shifted to microglia, OLGs and neurons. The distinct cellular proportions of A2B5-positive cells at P7 and P250 prevented further analysis on age-related differences between

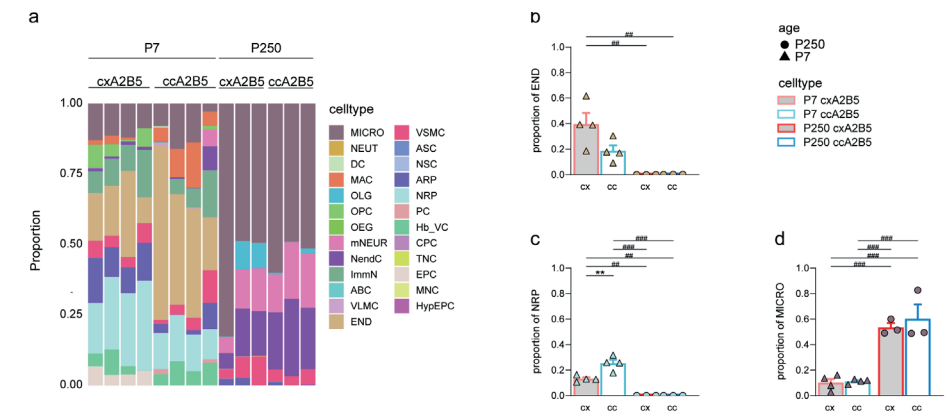


**Figure 4.** Deconvolution by SCDC suggests that different CNS cell types are bound by antibody A2B5 at P7 and P250. A2B5-positive cells (A2B5) were freshly isolated from the cortex (cxA2B5) and corpus callosum (ccA2B5) from postnatal days 7 (P7) and 250 (P250) rats using magnetic beads coupled to antibody A2B5. Antibody A2B5 binds c-series gangliosides and glycoproteins expressing the structure Neu5Acalpha2-->8Neu5Acalpha2-->8Neu5Acalpha-->. Four (P7) or three (P250) biological replicates were subjected to bulk 3'-RNA sequencing. Obtained data were deconvoluted by SCDC<sup>506</sup> using murine single-cell RNAseq data of Ximerakis and co-workers<sup>507</sup>. (a-i) Deconvolution of transcriptomic data using SCDC to estimate the proportions of central nervous system cell types in bulk RNAseq samples, shown are the relative proportions per group (a). The relative proportions of the indicated cell types in the biological replicates are shown in b-i. Bars represent average proportion per group. Error bars indicate standard error of the mean (SEM). Dots represent individual data points. Statistical analysis was performed using a one-way ANOVA with a Tukey post-test to compare the relative cell proportion between all groups. P-values of <0.05, <0.01, and <0.001 were considered significant and indicated with \*, \*\* or \*\*\* respectively. Note that SCDC reveals that, irrespective of region, P7 A2B5 consist of 13 different CNS cell types, including endothelial cells (END, a,b), neural restricted progenitor cells (NRP, a,c), microglia (MICRO, a,d), oligodendrocyte progenitor cells (OPC, a,e), and astrocyte restricted progenitors cells (ARP, a,f), while in P250 A2B5 6 CNS cell types were distinguished, including microglia (MICRO, a,c), mature neuron (mNEUR, a,g), neuroendocrine cells (NendC, a,h), oligodendrocytes (OLG, a,i). Neut, neutrophils; DC, dendritic cells; MAC, macrophages; OEG, olfactory ensheathing glia (OEG); immN, immature neurons; ABC, arachnoid barrier cells; VLMC, vascular and leptomeningeal cells; VSMC, vascular smooth muscle cells; ASC, astrocytes; NSC, neural stem cells; PC, pericytes; Hb\_VC, hemoglobin-expressing vascular cells; CPC, choroid plexus epithelial cells; TNC, tanocytes; EPC, ependymocytes; MNC, monocytes; HypEPC, hypendemat cells.

A2B5-positive cells of cx or cc. However, as the relative cellular composition of A2B5 positive cells at either age were quite similar, we next investigated how A2B5-positive cells were affected by region the same age.

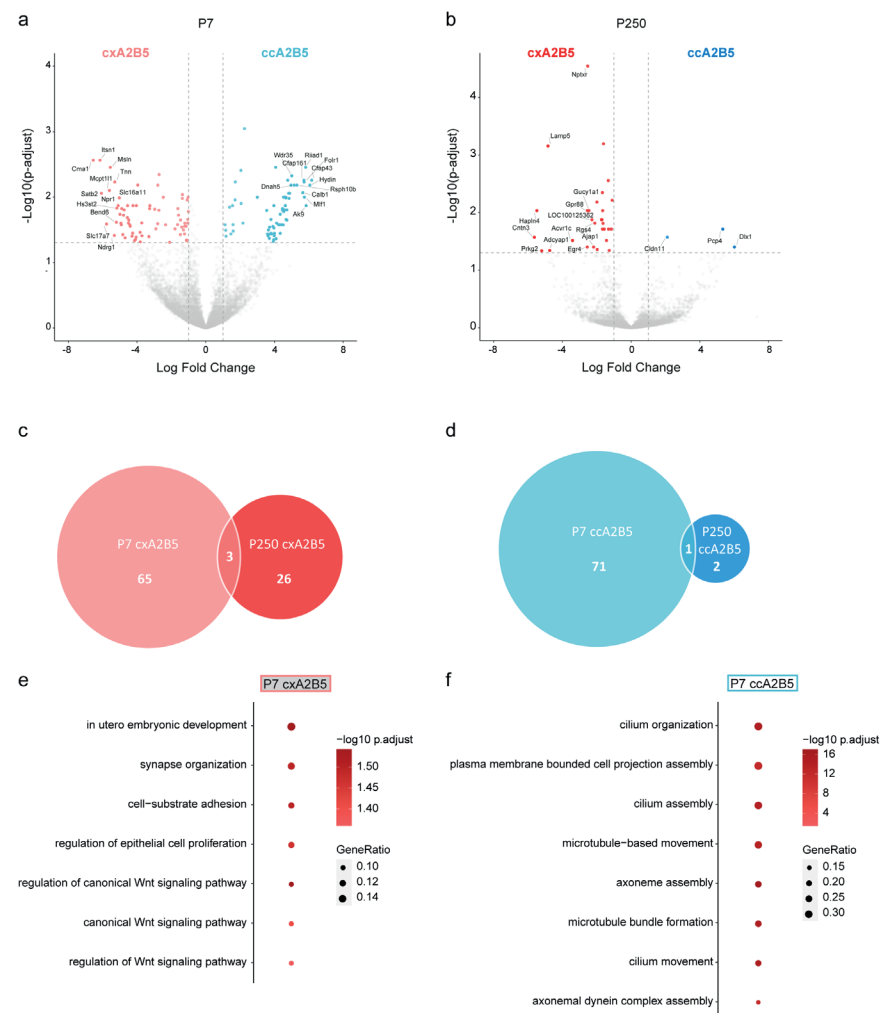


**Figure 5.** Regional transcriptomic differences between A2B5-positive cells of cortex and corpus callosum. A2B5-positive cells (A2B5) were freshly isolated from the cortex (cxA2B5) and corpus callosum (ccA2B5) from postnatal days 7 (P7) and 250 (P250) rats using magnetic beads coupled to antibody A2B5. Antibody A2B5 binds c-series gangliosides and glycoproteins expressing the structure Neu5Acalpha2-->8Neu5Acalpha2-->8Neu5Acalpha-->. Four (P7) and three (P250) biological replicates were subjected to bulk 3'-RNA sequencing. **(a,b)** Volcano plot showing the fold changes of gene expression (x axis log<sub>2</sub> scale) and their significance (y axis log<sub>10</sub> scale). The colored dots indicate differentially expressed genes (DEGs) between cxA2B5 and ccA2B5 at P7 **(a)** and P250 **(b)** as defined by a log<sub>2</sub> fold change > 1 and an adjusted p-value < 0.05. The grey dots represent genes that are not differentially expressed. **(c,d)** Venn diagrams displaying the total number of distinct and common overlapping DEGs between P7 A2B5 and P250 A2B5 in cx **(c)** and cc **(d)**. **(e,f)** Gene Ontology (GO) analysis of the DEGs that are more abundant in P7 cxA2B5 **(e)** and P7ccA2B5 **(f)**. The color of the dot represents the enrichment score ( $-\log_{10} \text{p-adjusted}$ ) and the size of the dot the gene ratio. Gene ratio is defined as the number of genes enriched in the data divided by the total number of genes associated

with the GO term. Note that DEGs related to functions as 'synapse organization' and 'canonical wnt signaling' are enriched in P7 cxA2B5, and 'cilium organization' and 'cilium assembly' in P7 ccA2B5.

### Transcriptomic differences between cortex and corpus callosum A2B5-positive cells

To obtain more insight in the discrete transcriptomic signatures of A2B5-positive cells from cx and cc, we performed differential gene expression analysis<sup>508</sup>. Differentially expressed genes were defined as genes with an absolute log<sub>2</sub> fold change greater than 1 and an adjusted p-value smaller than 0.05. Of the 9503 genes detected, 140 genes were differentially expressed between P7 cx and cc, of which 72 were more abundantly expressed in cc and 68 in cx (Fig. 5a, Table S1,2). Between P250 cx and cc samples, 32 DEGs were detected, of which 3 were more abundantly expressed in cc and 29 in cx (Fig. 5b, Table S3,4). The 3 DEGs enriched in P250 ccA2B5 included *Dlx1*, a gene reported to prevent differentiation of neural progenitors into OPCs<sup>509</sup>, *Cldnu*, a blood-brain barrier marker, and *Pcp4* a regulator of calmodulin activity and potentially involved in neuronal differentiation<sup>510</sup>. To examine a putative regional identity of A2B5-positive cells that is independent of age, we compared cxA2B5 and ccA2B5 at both P7 and P250. Of the 68 DEGs that were more abundantly expressed in P7 cx, and the 29 DEGs enriched in P250 cx, 3 genes overlapped (Fig. 5c, Table S1,3), including *Mef2c*, *Rgs4* and *Tmem130*. Only 1 gene, *Dlx1*, was enriched in both P7 and P250 ccA2B5 samples (Fig. 5d, Table S2,4). To determine in which biological processes the identified DEGs were involved, Gene Ontology (GO) analysis was performed. GO annotation of the 65 DEGs uniquely enriched in P7 cxA2B5 indicated involvement in 'synapse organization' and 'canonical Wnt signaling' (Fig. 5a,e, Table S1). Although no statistically significant different GO terms were associated with the 26 DEGs uniquely enriched in P250 cxA2B5, the DEGs *Gpr88*, *Gucy1a3*, *Bdnf*, *Neurl1* and *Adcyap1* (Table S3) are involved in 'synapse organization'. GO annotation further revealed that in P7 ccA2B5, genes involved in 'cilium organization' and 'cilium assembly' were more abundantly expressed, including *Hydin*, *Cfap161*, *Cfap43*, *Dnah5* and *Ak9* (Fig. 5a,f, Table S2). A gene interaction network of GO terms and related genes that are more abundantly expressed in P7 ccA2B5 are visualized in Fig. S3, demonstrating that some GO terms share a number of genes. In conclusion, these data indicate that A2B5-positive cells in P7 cx and P7 cc, and to a lesser extent in P250 cx and P250 cc, are involved in different biological processes.



## Discussion

Remyelination efficiency depends on region and age both in human and rodents<sup>24,26,27,45,46</sup>. Surface binding of the antibody A2B5 has been used to characterize and isolate cells from fetal, neonatal and adult human and rodent brain tissue as these cells are able to (re)myelinate axons in the adult CNS<sup>47,64,491-494</sup>. To obtain more insight in why remyelination is more efficient in GM than in WM, and decreases with age, we compared the transcriptomic profile of *ex vivo* isolated A2B5-positive cells of the cortex and corpus callosum at P7. At P7, developmental myelination is ongoing, while at P250 remyelination becomes less efficient<sup>46</sup>. Our comparative transcriptional profiling based on bulk RNAseq uncovered regional differences in the transcriptomic profiles of A2B5-positive cells from cx and cc at the same age. Analysis of lineage specific markers revealed that, although A2B5-immunogenicity is a well-known trait of OPCs, genetic markers of OLG maturation stages and the oligodendrocyte lineage cells were not among the most abundantly expressed marker genes in A2B5-positive cells. Deconvolution confirmed that, based on gene expression, A2B5-positive cells formed a heterogeneous population of various cell types of which the cellular composition most strongly differed between P7 and P250 and less between regions at the same age. P7 A2B5 consist mostly of progenitor cells and endothelial cells, while the major cell proportions of P250 A2B5 were OLGs, microglia and neurons. Notably, as the transcriptome of OPCs in the adult brain is more similar to mature OLGs than to neonatal OPCs<sup>57</sup>, the cellular proportion assigned as OLGs may include adult OPCs. Hence, our findings indicate that A2B5 binding was not restricted to glia progenitor cells and the expression of genetic cell markers of A2B5-positive cells shifted with age in the healthy rat brain. While the cell proportions marginally differ between region at the same age, cxA2B5 and ccA2B5 do have distinct transcriptomic profiles, and given the remyelination potential of A2B5-positive cells, this may contribute to regional differences in remyelination efficiency.

Currently it is not clear whether the cellular composition of A2B5-positive cells, based on gene expression levels, reflects multiple CNS cell types that show age-specific A2B5 immunogenicity or that A2B5-positive cells comprise multipotent progenitor cells having genetic hallmarks of different cell types. Thus, the unforeseen high abundance of transcripts of microglia-specific markers in P250 A2B5 may indicate that microglia

acquire A2B5-immunoreactivity with age *in vivo*, similarly to what has been reported that microglia become immunoreactive for the OPC-marker NG2 upon aging<sup>321,511,512</sup>. Notably, NG2 immunoreactivity of microglia has also been described in the fetal brain<sup>513</sup>, and in primary microglia obtained from the adult CNS<sup>514</sup>. In addition, in the SVZ of fetal human telencephalon, progenitors exist that co-express microglia and OPC markers<sup>515</sup>. On the other hand, fluorescence-activated cell sorting (FACS) analysis of A2B5-sorted cells of the rat and human adult brain identifies variable percentages of A2B5-positive/CD11b-positive cells ranging from 1 to 26%<sup>47,498,516</sup>. It cannot be excluded that given their reactivity and sensitivity to environmental signals, microglia may readily lose their A2B5 surface epitope following enzymatic tissue digestion and cell isolation, resulting in an underestimated percentage of microglia. Whether the A2B5 epitope resides on the surface of microglia *in vivo* in P250 brain and not P7 rat brain remains to be determined. Amoeboid ganglioside GD3-expressing microglia are present in regions of oligodendrogenesis<sup>517</sup>, and GD3 surface expression in microglia is increased upon inflammation<sup>518,519</sup>. Hence, OPCs and microglia may have an overlap in expression of commonly used marker proteins. Of relevance, at defined culture conditions, a subset of microglia can function as multipotent progenitors, generating neurons, astrocytes and OLGs<sup>514</sup>. Likely, environmental conditions determine the outcome of the cellular lineage and function of these progenitors. Indeed, a single-cell RNAseq study in EAE, an animal model that reflects inflammatory aspects of MS, revealed that isolation of PDGFR $\alpha$ -positive cells in the spinal cord included a subpopulation of microglial like-cells in EAE, but not control mice, that are distinct from oligodendrocyte lineage cells<sup>29</sup>. In addition, the microenvironment becomes stiffer with age, and A2B5-positive cells isolated from the aged adult brain re-acquire properties of A2B5-positive cells isolated from young adult brain when plated in a less stiff environment<sup>520</sup>. Conversely, it is tempting to suggest that microglia are formed from A2B5-positive progenitors. For example, microglia that repopulate white matter after microglia necroptosis during remyelination, are spontaneously produced from progenitor cells expressing the neural stem cell marker nestin<sup>521</sup>. Our findings further indicated that irrespective of region, P7 A2B5 consist of a high proportion of endothelial cells that are located at the vasculature. This finding is in line with previous immunohistochemical observations that antibody A2B5 also lightly binds to gangliosides GD1a and GM3<sup>522</sup> expressed on endothelium<sup>523</sup>. However, this does not explain the relative lower abundance of the relative endothelial cell proportion of P250 A2B5

compared to P7 A2B5, as GD1a surface expression on aging endothelium remains stable<sup>523</sup>. Single-cell RNAseq studies along with immunohistochemical analysis and *in vitro* experiments at defined culture conditions will provide more insight in the identity and plasticity of the distinct A2B5-positive cell types.

A2B5-positive cells are distributed throughout the brain, and when isolated from developing or adult rat or human, readily differentiate *in vitro* into OLGs, neurons or astrocytes dependent on culture conditions<sup>147,492,499,502,513,524,525</sup>. Similarly, many studies have addressed that when transplanted into dysmyelinated shiverer mice<sup>64</sup> or demyelinated WM areas<sup>493,494,520</sup> A2B5-positive cells ensheath and myelinate axons. Although the role of endogenous A2B5-positive cells in remyelination *in vivo* remains to be determined, our comparative transcriptomic profiling indicated age-specific regional heterogeneity in A2B5-positive cells of the P7 and P250 rat brain. Thus, while P7 cxA2B5 had a strong differential transcriptomic signature for ‘synapse organization’ and ‘canonical wnt signaling’, the differential transcriptomic signature of their P7 cc counterparts relates to ‘cilium organization’ and ‘cilium assembly’. Activation of canonical Wnt signaling prevents OPC differentiation<sup>419,420,526</sup> and synaptic regulation of developmental myelination has been described<sup>527</sup>. DEGs that relate to ‘synapse organization’ were also more abundant in P250 cxA2B5 than P250 ccA2B5, while relative cell type proportions -including neurons- were similar, indicating a regional specialized role of A2B5-positive cells in synapse organization. The relevance of distinct roles of A2B5-positive cells in cx and cc in the homeostatic middle-aged brain in the context of their response to demyelinating injury warrants further investigation. Notably, axon-OPC contacts are observed in active MS lesions, while downregulation of axon-OPC synapses play a role in OPC proliferation early after demyelination<sup>528</sup>. In addition, murine OPCs<sup>79,529</sup> and oligodendrocyte lineage cells<sup>78</sup> have been implicated to be able to modulate synaptic signaling, and human OPCs from WM are enriched in synapse-related GO terms when compared to other wmOLG maturation stages<sup>20</sup>.

Taken together, the age-specific regional differences and cellular diversity in transcriptomic A2B5 signatures may contribute to differences in remyelination efficiency in the cx and cc. Yet, based on their transcriptomic signature, antibody A2B5 may bind to the surface of different CNS cell types, including endothelial cells at P7 and

microglia at P250. Therefore, while antibody A2B5-bound magnetic beads or FACS sorting based on antibody A2B5 surface epitopes are used to isolate OPCs from rat and human brain tissue, for further research investigating the role of OPCs in remyelination, it is recommendable to further purify the A2B5-positive population either by negative selection using other cell type markers, or positive selection using another OPC cell surface marker. This OPC marker should not be PDGFR $\alpha$  or NG2, but for example brevican for human OPCs<sup>20</sup> or as adult OPCs are more mature than neonatal OPCs<sup>57,102</sup>, the late OPC surface markers sulfatide (recognized by antibody O4), lumican or clusterin<sup>530</sup>. Also, region-specific marker expression should be taken into account, as for example the more mature OPC marker G-protein coupled receptor 17 is expressed on OPCs upon demyelination in the corpus callosum, but not in cortex<sup>240</sup>. Taking into account age and region-specific variation of OPCs will further contribute to our understanding of differences in remyelination, and the failure thereof in the aging CNS and demyelinating diseases such as MS.

## Methods

### *Ex vivo* isolation of A2B5-positive cells

Animal experimental protocols were approved by the Institutional Animal Care and Use Committee of the University of Groningen (the Netherlands). All experiments were carried out according to local and national experimental animal regulations and guidelines. Brains were obtained from male and female Wistar rat littermates for postnatal day 7 (P7), and 4 mixed female and male (2:2) Wistar rats for P250 brain tissue. After removal of meninges, cortex (cx) and corpus callosum (cc) were dissected from each brain and pooled. Tissue was digested in papain digestion mix (240 µg/ml L-cysteine (Sigma-Aldrich, cat. no. C7477), 40 µg/ml DNase I (Roche, cat. no. 10104159001), 30U papain from papaya latex (Sigma-Aldrich, cat. no. P3125) in DMEM) for 50-60 minutes at 37°C. Enzymatic digestion was stopped by the addition of OVO (40 µg/ml DNase I, 1 mg/ml trypsin inhibitor (Sigma-Aldrich, cat. no. T6522), 50 µg/ml bovine serum albumin (BSA; Sigma-Aldrich, cat. no. A4919) in L15 medium (Sigma-Aldrich, cat. no. L4386)) twice for 3 minutes. For P250 tissue, myelin was then removed using Percoll gradient centrifugation. In brief, cells were resuspended in 15ml 22% Percoll buffer onto which 3ml PBS was gently added. The suspension was centrifuged for 20min at 950 g at 4°C. The supernatant, containing a myelin-enriched interlayer, was discarded. Red blood cells were lysed using red blood cell lysis buffer according to manufacturer's instructions (Biolegend, cat. no. 420301). Cells were resuspended in MACS buffer (0.5% BSA in PBS) at 4°C after which microbeads conjugated to monoclonal mouse antibody A2B5 of the IgM isotype (Miltenyi Biotech, cat. no. 130-093-388) were added. Magnetic sorting was performed using MS column (Miltenyi Biotech, cat. no. 130-042-201) selection.  $4 \times 10^5$  antibody A2B5-bound cells of cx and cc were resuspended in RNAlprotect (Qiagen, cat. no. 76526) and stored at -80°C until further processing. Four biological replicates were produced from P7 neonatal rats of four different litters, and three biological replicates were produced from 12 P250 middle-aged rats. For immunocytochemical analysis,  $4 \times 10^4$  isolated cells were plated on poly-L-lysine coated glass slides in Sato medium<sup>144</sup>.

## Immunocytochemistry

Antibody A2B5 cell surface staining was stained on living cells at 4°C. Cells were incubated in 4% BSA in PBS for 10 minutes to block non-specific antibody binding. Cells were washed two times with PBS (4°C) after which cells were incubated for 30 minutes with A2B5 (1:5; kind gift of Dr. Thijs Lopez-Cardozo, Utrecht, the Netherlands). After two washes with PBS (4°C), cells were incubated with TRITC-conjugated IgM antibodies (1:50; Jackson ImmunoResearch). Cells were fixed with 4% paraformaldehyde (PFA) in PBS for 20 minutes at room temperature, followed by incubation with DAPI (1 µg/ml, Sigma, cat.no. 32670) for 15 minutes at room temperature to visualize nuclei. For double labeling with Iba1, cells were permeabilized using ice-cold methanol for 10 minutes. Non-specific antibody binding was blocked with 4% BSA in PBS for 30min. Cells were incubated with anti-Iba1 antibodies (1:250; Abcam cat. no. ab5076) for 1 hour at room temperature. After three times washing with PBS, FITC-conjugated anti-rabbit antibodies (1:50; Jackson ImmunoResearch) and DAPI were added and incubated for 30 minutes at room temperature. After three times washing with PBS, cells were mounted in Dako mounting medium (Dako, cat. no. S3025) to prevent image fading. Cells were visualized with a conventional immunofluorescence microscope (Leica DMI 6000B with Leica Application Suite Advanced Fluorescence software).

## Gene expression

mRNA was isolated using the RNeasy Plus Micro Kit (Qiagen, cat. no. 74034) according to manufacturer's instructions. The quantity and quality of the mRNA was assessed using an Experion electrophoresis system (Bio-Rad Laboratories). The RIN-values of all samples were higher than 8.0.

## Data preprocessing

The Lexogen QuantSeq 3'mRNA-Seq Library Prep kit for Illumina was used according manufacturer's instructions for library preparation. Samples were sequenced on the Illumina NexSeq-500. Data was processed using MOLGENIS compute (version NGS\_RNA/3.2.5). Quality control was performed on the raw fastq files with fastQC (0.11.3). Alignment of the sequenced reads was done with HiSat (0.1.5) against the

*Rattus norvegicus* genome (38.82) allowing 2 mismatches. The aligned data was sorted with samtools (1.2). Ultimately, data was quantified with the use of HTSeq (0.6.1p1) using the following parameters: --stranded=no and --mode=union.

#### *Differential Gene Expression (DEG) analysis*

Lowly expressed counts genes were filtered with two complementary methods. First, genes were filtered using a data-adaptive flag method (DAFS) to estimate the optimal cut-off between lowly and highly expressed genes for each sample<sup>531</sup>. Second, because there were initially too many lowly expressed genes in the voom mean-variance plot, additional filtering was performed with the filterByExpr() function with default settings (EdgeR, version 3.28.1). Bulk RNAseq differential expression analysis was conducted by fitting a linear model using the R package limma (version 3.42.2)<sup>532</sup>. We applied the limma-voom<sup>508</sup> normalization and followed the statistical guidelines in limma's userguide. Brain regions were compared with moderated t-tests using the eBayes() function. Rat ID was treated as random intercept using the duplicateCorrelation() function. Genes with a log<sub>2</sub> fold change > 1 and adjusted p-value < 0.05 were reported as differentially expressed. Principal Component Analysis was conducted with the prcomp() function using limma-voom normalized counts of the top 500 most variable genes. GO enrichment analysis for differentially expressed genes was computed with the clusterProfiler package (version 3.14.3) using the rat genome 'org.Rn.eg.db' as background, pvalueCutoff = 0.05, pAdjustMethod = 'BH' and qvalueCutoff = 0.1 in the enrichGO() function<sup>533</sup>. Visualizations were made with R package ggplot2 (v3.3.0).

#### *Deconvolution*

Deconvolution was performed using BRETIGEA and SCDC. BRETIGEA is an R package that composed marker gene sets for brain cell types using several independent human and mouse single-cell RNA datasets, which can then be used to estimate cell type proportions in RNA datasets<sup>505</sup>. nMarker was set at 50. To deconvolve the bulk RNAseq data, we included all genes with expression levels in counts per million. Cell type proportions were determined by calculating the differences between relative cell type proportion estimate values. SCDC leverages cell type specific gene expres-

sion from single-cell RNA datasets to decompose bulk RNAseq into cell type proportions<sup>506</sup>. A single cell RNAseq dataset of mouse brain by Ximerakis et al.<sup>507</sup> was used as reference to deconvolve the bulk RNAseq by applying the SCDC\_prop() function with default settings.

#### **Statistical analyses**

Data are obtained from four (P7) or three (P250) biological replicates and expressed as means ± standard error of the mean (SEM). Statistical analyses were performed using GraphPad Prism 6.0. For each gene individually, we performed a one-way ANOVA with a Tukey *post-hoc* test to compare relative cell type specific marker proportions between experimental groups. P-values of <0.05, <0.01, and <0.001 were considered significant and indicated with \*, \*\*, \*\*\* (difference between regions) or #, ##, ### (difference between age), respectively.

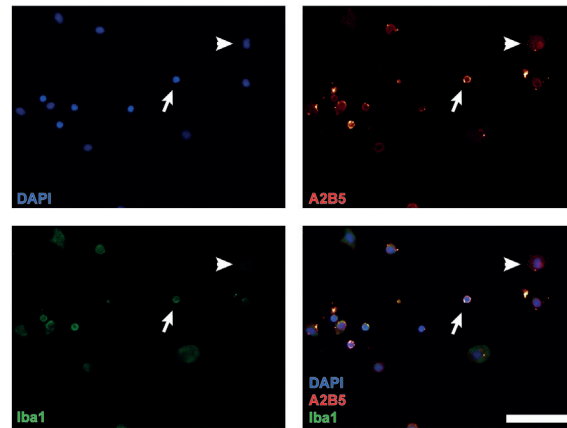


**Figure S1.** *Ex vivo* isolated A2B5-positive cells from P250 rat brain co-label with the microglia marker Iba1. A2B5-positive cells (A2B5) were freshly isolated from the cortex (cxA2B5) and corpus callosum (ccA2B5) from 250-day old rats using magnetic beads coupled to antibody A2B5. Antibody A2B5 binds c-series gangliosides and glycoproteins expressing the structure Neu5Acalpha2-->8Neu5Acalpha2-->8Neu5Acalpha-->. Obtained cells were plated for 1 hour on poly-L-lysine coated glass slides. Cells were surface stained with antibody A2B5 (red), followed by an intracellular staining of the microglia marker Iba1 (green). Nuclei are stained with DAPI (blue). Note the presence of A2B5-positive/Iba1-positive cells (arrow) and A2B5-positive/Iba1-negative cells (arrowhead). Scale bar is 50  $\mu$ m.

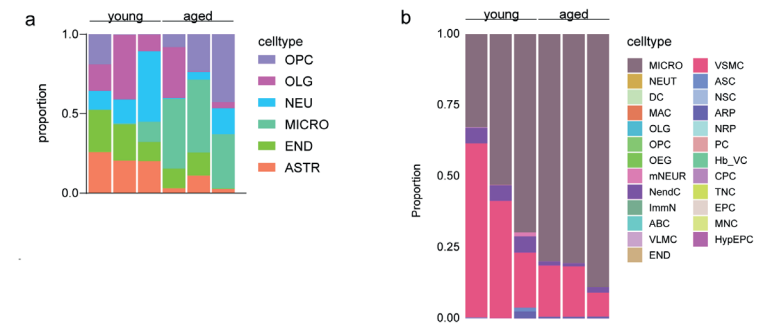


**Figure S2.** Deconvolution of transcriptomic data of A2B5-sorted cells by Neuman et al.<sup>47</sup> suggests that different cell types are present within the A2B5-positive cell population. Neumann et al. performed transcriptomic analysis on A2B5-positive cells from the young adult (P60-90) and aged (P600-720) total rat brain (GSE134765). Deconvolution of this transcriptomic data by the R package BRETIGEA<sup>505</sup> is shown **a** and by SCDC<sup>506</sup> using the murine single-cell dataset of Ximerakis and co-workers<sup>507</sup> in **b**. An estimation of the relative proportions of indicated cell types in bulk RNAseq samples in each independent sample is shown. Note that with this independent transcriptomic data set, A2B5-positive cells also consist of different central nervous system resident cell types proportions.

